Published in final edited form as:
Sci Transl Med. 2009 October 21; 1(3): 3ra7. doi:10.1126/scitranslmed.3000139.

Radioprotection in Normal Tissue and Delayed Tumor Growth by Blockade of CD47 Signaling

Justin B. Maxhimer[1,3], **David R. Soto-Pantoja**[1], **Lisa A Ridnour**[2], **Hubert B. Shih**[1,4], **William G. DeGraff**[2], **Maria Tsokos**[1], **David A. Wink**[2], **Jeff S. Isenberg**[5], and **David D. Roberts**[1]

[1] Laboratory of Pathology, Center for Cancer Research, National Cancer Institute, National Institutes of Health, Bethesda, Maryland 20892

[2] Radiation Biology Branch, Center for Cancer Research, National Cancer Institute, National Institutes of Health, Bethesda, Maryland 20892

[3] The Johns Hopkins Medical Institutions, Department of Surgery, Baltimore, Maryland 21287

[4] Howard Hughes Medical Institute–National Institutes of Health Research Scholars Program, Bethesda, MD 20814

[5] Vascular Medicine Institute of the University of Pittsburgh and the Department of Medicine, University of Pittsburgh School of Medicine, Pittsburgh, PA 15261

Abstract

Radiation-induced damage of normal tissues restricts the therapeutic doses of ionizing radiation that can be delivered to tumors and thereby limits the effectiveness of radiotherapy. Thrombospondin-1 signaling through its cell surface receptor CD47 limits recovery from several types of stress, and mice lacking either gene are profoundly resistant to radiation injury. We describe strategies to protect normal tissues from radiation damage using CD47 or thrombospondin-1 antibodies, a CD47-binding peptide, or antisense suppression of CD47. A morpholino oligonucleotide targeting CD47 confers radioresistance to human endothelial cells in vitro and protects soft tissue, bone marrow, and tumor-associated leukocytes in irradiated mice. In contrast, CD47 suppression in mice bearing melanoma or squamous lung tumors prior to irradiation result in 89% and 71% smaller tumors, respectively. Thus, inhibiting CD47 signaling maintains the viability of normal tissues following irradiation while increasing the radiosensitivity of tumors.

Introduction

Irradiation is part of the therapeutic plan for over half of all cancer patients (1). The major side effects associated with this treatment result from radiation-induced damage to normal tissue (2,3), including acute destruction of rapidly proliferating cells in radiosensitive tissues (lymphoid organs, bone marrow, intestinal crypts, testes, and ovaries) and long term fibrotic damage to soft tissues that progressively limit their function. Although the use of precise fields and accurate dose planning can limit this damage to adjacent tissues, it still occurs in most patients and ultimately limits the effective radiation dose that can be delivered to a tumor (4–6).

Address correspondence to: David D. Roberts, Ph.D., National Institutes of Health, Building 10 Room 2A33, 10 Center Drive, MSC1500, Bethesda, Maryland, 20892-1500, droberts@helix.nih.gov.

Summary
Suppression of CD47 expression protects normal tissue from radiation injury and simultaneously enhances the activity of ionizing radiation to delay tumor growth.

Ionizing radiation causes genomic instability, cell death, fibrosis, and tissue necrosis (7). Some radiation-induced injuries to normal tissue result from direct damage to macromolecules,, but most damage arises from generation of reactive oxygen and nitrogen species that cause DNA double-stranded breaks, producing chromosomal rearrangements and resulting in cell cycle arrest and cell death (8–11).

The important role of free radicals in mediating radiation injury has been exploited to develop radiosensitizers that increase radical damage and the responses of tumors to ablative radiotherapy (12). Conversely, efforts to devise therapies that scavenge free radicals to selectively protect normal tissue from the damaging effects of ionizing radiation have shown success (13), but their clinical utility is diminished either by drug toxicity or by their protecting tumors as well as normal tissue from irradiation. For example, the prodrug Amifostine generates an active free thiol metabolite that scavenges free radicals and is an approved radioprotectant for radiotherapy of head and neck cancer that reduces mucositis and improves complete response rates (14). However, the selectivity of Amifostine for normal tissue remains controversial, and reports of tumor radioprotection along with numerous side effects have limited its broader clinical use (15,16). A number of additional radioprotection approaches, such as scavenging free radicals by increasing Mn-superoxide dismutase levels, are currently in preclinical development (17).

Thrombospondin-1 (TSP1), a glycoprotein produced and secreted by a variety of cell types in response to growth factors, inflammation, and other forms of injury, can both increase and decrease endothelial and vascular smooth muscle cell proliferation, motility and adhesion, while limiting endothelial cell survival (18,19). TSP1, through its necessary receptor CD47, limits the pro-survival effects of nitric oxide (NO) in vascular cells and tissues (20,21). TSP1 inhibits the canonical NO pathway at multiple levels including its main cellular target soluble guanylate cyclase and downstream at cGMP-dependent protein kinase (18,20,22). TSP1 and CD47 null mice and primary cells cultured from these mice show increased physiologic NO signaling and dramatically increased resistance to tissue death from ischemia and ischemia-reperfusion injuries (23,24).

Consistent with the known radioprotective activity of NO donors (25,26), the absence of TSP1 or CD47 also confers near complete resistance to high dose radiation injury in primary null cells and in the whole animal (27). These findings suggested that therapeutically blocking TSP1-CD47 interactions in wild type animals could confer similar radioprotection of normal tissue. Here we validate several such approaches to radioprotect human cells in vitro and examine their radioprotective activities in healthy and tumor-bearing mice.

Results

Radioprotection of human endothelial cells by targeting TSP1 or CD47

The profound radioresistance of primary vascular cells cultured from TSP1 and CD47 null mice demonstrates that this effect is cell autonomous (27). Thus, we tested primary human umbilical vein endothelial cells (HUVEC) that express both TSP1 and CD47 to investigate whether therapeutic targeting of TSP1 or CD47 could confer similar radioprotection. HUVEC showed dramatically increased radioresistance when treated with antibodies to TSP1 (clone A6.1) or its receptor CD47 (clone B6H12), both of which block signaling through this receptor (21,28), and mitochondrial function in the treated cells was preserved at up to 40 Gy (Fig. 1A, B). A CD47 binding peptide (7N3) that inhibits TSP1 binding to CD47 (29) was less efficacious (Fig. 1C), but at higher radiation doses it still enhanced cell survival after irradiation relative to the control peptide 604 (Fig. 1D).

Although viable, the above data do not show that the treated endothelial cells can proliferate after irradiation. Therefore, we measured bromodeoxyuridine (BrdU) incorporation into newly synthesized DNA in HUVEC treated with increasing doses of A6.1, B6H12 antibodies and the 7N3 peptide (Fig. 1E, 1F, 1G, respectively) prior to single dose irradiation at 40 Gy. Irradiation of untreated HUVEC caused a reduction in BrdU uptake, but treatment with A6.1 and B6H12 dose-dependently increased BrdU incorporation almost to that of the un-irradiated control. Peptide 7N3 also enhanced BrdU incorporation in irradiated HUVEC, but less effectively than the antibodies. Together, these results indicate that blockade of TSP1 or CD47 allows survival and sustained proliferation of endothelial cells after irradiation.

Previous reports showed that suppression of CD47 expression in cells and tissues is sufficient to enhance physiologic NO signaling and confer tissue protection to ischemia (30,31). Similarly, an antisense CD47 morpholino rendered HUVEC resistant to radiation-induced cell death when compared to untreated, mismatched morpholino, and morpholino delivery vehicle (Endoporter) controls (Fig. 1H) ($P < 0.05$). This radioprotective effect is specific to TSP1-CD47 signaling in that HUVEC treated with an antisense morpholino specific for another TSP1 receptor, CD36, showed a decrease in cellular viability similar to that of untreated cells and cells treated with the corresponding mismatched control morpholino (Fig 1I).

TSP1/CD47 blockade maintains proliferative capacity in irradiated endothelial cells

Tissue health requires the ability to repair and replace damaged structures through cell proliferation. Proliferative capacities are typically lost in normal tissues following ionizing radiation injury. We therefore determined whether therapeutic targeting of TSP1/CD47 preserved the proliferative capabilities of human vascular cells. DNA synthesis following irradiation in untreated cells progressively decreased over 1 week (Fig. 2A). Pretreatment with the CD47 morpholino, but not with vehicle or a mismatched control morpholino, maintained proliferation in cells exposed to radiation over the same time period (Fig. 2A) ($P < 0.05$). Enhanced DNA synthesis was also seen under the same conditions with blocking antibodies against either TSP1 or CD47 (Fig. 2B) ($P < 0.05$). These results were consistent with our previous observations that primary murine TSP1 and CD47-null vascular cells maintain their proliferative capacity even after irradiation at 40 Gy (27).

Increased NO or cGMP is not sufficient for radioprotection

Administration of the slow releasing NO donor diethyltriamine NONOate (DETA/NO) has been associated with increased survival in irradiated hamster fibroblasts (25) and whole body irradiation in mice (26). TSP1, via CD47, limits physiologic NO signaling in vascular cells and tissues of several mammalian species including mice and pigs (20,31,32), suggesting that the radioprotection obtained by suppressing CD47 expression results from enhanced NO signaling. However, treatment with DETA/NO (Fig. 3A) or a cell permeable cGMP analog (Fig. 3B) did not confer a significant survival advantage to irradiated HUVEC. Conversely, non-selective inhibition of endogenous NO production by NO synthases with L-NAME did not significantly increase cell death after irradiation (Fig. 3C) and did not prevent treatment with the CD47 morpholino from enhancing cell survival (Fig. 3C). Therefore, the radioprotection afforded by TSP1/CD47 targeting occurs in a largely NO-independent manner.

Tissue protection and decreased vasculopathy from radiation injury by antisense CD47 suppression

To test whether interference with TSP1 signaling through CD47 could confer radioprotection in vivo, we treated the right hindlimb of age and sex matched C57BL/6 wild type mice with a one-time 750 μl local injection into the muscle and soft tissues of the CD47 antisense morpholino oligonucleotide (10 μM in PBS), a mismatched control morpholino, or vehicle (PBS). Forty-eight hours later the animals received 25 Gy irradiation to the treated hindlimb.

At the end of 8 weeks, significant alopecia, dry and wet desquamation, and tissue ulceration with fibrous contracture of radiated hindlimbs was noted in mice pre-treated with the control morpholino or vehicle. In contrast, mice receiving the CD47 targeting morpholino showed less alopecia, ulceration, and desquamation at the end of 8 weeks (Fig. 4A, B). The hindlimbs of treated mice also showed less contracture due to fibrosis ($P < 0.04$) and remained more flexible and supple (Fig. 4C). The vasculature and in particular vascular endothelial cells are very sensitive to radiation (33–35). Following injury, vascular networks undergo a progressive fibrous obliteration, resulting in a loss of perfusion, ischemia, and tissue necrosis. Irradiated hindlimbs treated with the CD47 suppressing morpholino showed enhanced vascular perfusion in response to challenge with the fast releasing NO donor diethylamine NONOate (DEA/NO) assessed by laser Doppler imaging 8 weeks after irradiation (Fig. 4D upper panels, E). In contrast, vehicle-treated irradiated hindlimbs demonstrated an impaired response to this vasodilator (Fig. 4D lower panels, E). Therefore, the ability of an irradiated vascular bed to respond to a physiological vasodilator is preserved by suppression of CD47.

Reduced apoptosis in irradiated bone marrow and skeletal muscle through CD47 suppression

Control hindlimbs examined 24 h after irradiation showed the expected apoptosis response detected by terminal deoxynucleotidyl transferase dUTP nick end labeling (TUNEL) staining in bone marrow and skeletal muscle cells (Fig. 5A). In contrast, hindlimbs that received the CD47 morpholino demonstrated significantly less cell death in the skeletal muscle (36.0 ± 4 vs. 12.0 ± 1.0, n=5 for both groups Fig. 5A, B) ($P < 0.0001$). Based on examination of H&E stained sections after 8 weeks (results not shown), the increased survival of treated hindlimb skeletal muscle was comparable to that obtained in hindlimbs from CD47 null mice (27). Although bone marrow cells are among the most sensitive to radiation-induced death, reduced TUNEL staining after 24 h indicated that tissue protection by CD47 morpholino treatment extends to the bone marrow compartment (48.0 ± 3.7 vs. 25.6 ± 4.4 n=5 for both groups Fig. 5A, C) ($P < 0.0001$)..

CD47 suppression protects hematopoietic progenitors

To examine whether CD47 suppression preserves the proliferative capacity of bone marrow hematopoietic progenitor cells, bone marrow cells were harvested immediately after 10 Gy irradiation from the femurs of untreated mice or mice pretreated for 48 h with CD47 morpholino The cells were plated in methylcellulose medium containing appropriate growth factors to assess colony forming units (CFU) for erythroid (CFU-E), burst-forming unit-erythroid (BFU-E), granulocyte (CFU-G), macrophage (CFU-M), granulocyte/macrophage (CFU-GM), and granulocyte/erythroid/macrophage/megakaryocyte (CFU-GEMM) progenitors. Cultures derived from mice treated with CD47 morpholino showed 74 % more total CFU when compared to cultures of cells derived from mice treated with PBS (Fig. 5D) (191 ± 11 vs.109 ± 19, n = 5 for both groups). Thus, blockade of CD47 by morpholino treatment protects bone marrow progenitor cell clonogenic activity after irradiation, demonstrating the ability of such irradiated cells to undergo multiple cycles of cell division.

Radiation combined with CD47 suppression increases growth delay in two syngeneic murine tumor models

A major concern with any radioprotection strategy is that it will likewise enhance radio-resistance in tumors. Published results for syngeneic tumors implanted in TSP1 null mice demonstrated no loss in radiosensitivity in these tumors (27), but this does not address whether suppressing CD47 expression in the tumor would be radioprotective. Therefore, we implanted syngeneic B16 melanoma tumors into the thighs of C57BL/6 mice, treated them with the CD47 targeting morpholino or vehicle, and followed tumor growth rates after therapeutic irradiation

(10 Gy). As expected, vehicle control and tumor only groups demonstrated rapid tumor growth, with animals succumbing within 3–4 weeks. Treatment with the morpholino in the absence of irradiation only slightly delayed tumor growth. Irradiation alone resulted in the expected regrowth delay. In contrast, treatment of tumor-bearing limbs with the CD47 morpholino followed by irradiation dramatically delayed tumor re-growth relative to irradiation alone (Fig. 6A). Concurrent with an enhanced tumor response to radiation, TUNEL staining of muscle and bone marrow tissues adjacent to the tumor and within the field of radiation showed radiation-induced cell death, which was markedly decreased in mice treated with the CD47 morpholino (supplemental Fig. 1).

To determine whether this enhanced tumor response to ionizing radiation was unique to B16 melanoma or the C57BL/6 background, we conducted another study in C3H mice implanted into the hindlimb with a mouse squamous cell carcinoma (SCC VII). The same treatment and radiation schedules were used, and similar tumor growth delays relative to irradiation alone were seen in those mice treated with the CD47 morpholino (Fig. 6B).

Patient tumors are frequently not accessible for local injection, so we compared radiation-induced growth delays in SCC VII tumors treated locally or by intraperitoneal injection of CD47 morpholino (Fig. 6C). Growth delays were comparable for both treatment routes, consistent with previous reports of systemic activity of morpholino oligonucleotides (36). Therefore, local treatment is not required to achieve increased tumor responses to irradiation by CD47 suppression.

One possible explanation for this unexpected enhancement of tumor regrowth delay is that CD47 suppression confers increased radiosensitivity to the tumor cells. Analysis of isolated B16 melanoma cells exposed to irradiation (10 Gy), however, revealed a mild radioprotective effect for cell viability *in vitro* after treatment with either peptide 7N3 or CD47 morpholino when compared to untreated cells (Fig. 6D) ($P < 0.05$). Therefore, CD47 suppression results in a mild cell-autonomous increase in radio-resistance of this tumor cell line that cannot explain the large tumor growth delay seen *in vivo.*

Increased fibrosis, inflammatory response, and macrophage infiltration in tumors where CD47 is suppressed

Enhancement of anti-tumor immunity is another mechanism by which CD47 suppression could increase the sensitivity of tumors to radiation *in vivo*. Tumor cells are often infiltrated with inflammatory cells such as lymphocytes, neutrophils, macrophages, and mast cells. Depending on their differentiation state, tumor-infiltrating macrophages can either limit or support tumor growth (37–39). Killing of tumor cells by M1 differentiated macrophages involves phagocytosis, which is inhibited when the target cells express CD47 (40,41), suggesting that suppression of CD47 on either the tumor or infiltrating cells could affect tumor re-growth. H&E staining of B16 tumors from irradiated hindlimbs treated with the CD47 morpholino revealed greater fibrosis and necrotic response within the tumor parenchyma after radiation compared to irradiated tumors without treatment (Fig. 7A). As expected, tumors in irradiated untreated hindlimbs had increased numbers of inflammatory cells undergoing apoptosis (Fig. 7B center panel, D). In contrast, tumors treated with the CD47 morpholino prior to irradiation showed radioprotection of inflammatory cells associated with the tumor (59.8 ± 3.8 in the tumor + radiation group vs. 33.6 ± 5.2 in the tumor + radiation + CD47 morpholino group, n=5 in each group $P < 0.0001$) (Fig. 7B right panel, D). Concurrently, tissue staining for the macrophage marker CD68 showed increased positive staining in the periphery of those tumors subjected to CD47 suppression (28.4 ± 4.5 in the tumor + radiation group vs. 60.4 ± 6.2 in the tumor + radiation + CD47 morpholino group, n=5 in each group $P<0.0001$) (Fig. 7C, E). Therefore, the increased regrowth delay in irradiated tumor-bearing limbs treated with the

CD47 morpholino is associated with increased macrophage recruitment and/or survival, which may result in enhanced innate immune clearance of these irradiated tumors.

Discussion

These results demonstrate that temporary suppression of CD47 expression can protect normal tissues from damage by ionizing radiation. This protection is observed in the skin, muscle, and bone marrow of irradiated mouse hindlimbs. Consistent with previous results using TSP1 null and CD47 null murine vascular cells (27), inhibiting TSP1-CD47 signaling cell-autonomously protects human endothelial cells from radiation-induced death and preserves their proliferative capacity. Suppression of CD47 in vivo also preserves the proliferative capacity of hematopoietic progenitors in bone marrow. In addition to CD47 antisense suppression of CD47 expression, synthetic peptides and antibodies that inhibit TSP1 binding to CD47 (29) induce radioresistance *in vitro*. Although suppression of CD47 also confers a modest radioprotection to B16 melanoma cells *in vitro*, such radioprotection does not occur for B16 or SCC VII tumors *in vivo*. Rather, suppression of CD47 enhances the radiation-induced regrowth delay in two strains of mice bearing syngeneic melanoma or squamous lung carcinoma tumors, respectively. These results predict that therapeutic targeting of the TSP1/CD47 interaction would be an effective means to enhance tumor ablation by radiotherapy, while at the same time decreasing the harmful effects of radiation treatment on adjacent normal tissues. Our results further demonstrate that this selective radioprotection can be achieved by systemic delivery of the CD47 morpholino.

The mechanism for increased tumor radiosensitivity following CD47 suppression is not yet clear. Suppressing CD47 expression on B16 melanoma cells *in vitro* does not increase their intrinsic sensitivity to radiation, so the increased regrowth delay is not tumor cell autonomous. Previous studies suggest two explanations. One is that CD47 suppression protects tumor infiltrating leukocytes from killing by irradiation, and these may have enhanced cytotoxic activities against irradiated tumor cells with decreased CD47 expression (40,42,43). This hypothesis is supported by our observations that CD47 blockade protects tumor associated leukocytes against radiation-induced cell death in bone marrow and in irradiated tumors and by our previous observation that regrowth is also delayed after irradiation for B16 tumors grown in TSP1 null mice (27). Specifically, the number of tumor-associated macrophages is increased following CD47 blockade. Recently, ionizing radiation was shown to induce the secretion by cancer cells of proinflammatory chemotactic factors that recruit anti-tumor effector T cells and aid in the anti-tumor immune response (44). In addition to killing tumor cells, local irradiation induces apoptotic cell death of tumor-associated macrophages and T cells within. Thus, radiation directly ablates the tumor but simultaneously compromises host anti-tumor immunity (45). If CD47 suppression preferentially protects tumor-associated macrophages, this could account for our observation of increased tumor associated macrophages for irradiated tumors pretreated with the CD47 morpholino.

A second potential mechanism involves the effect of increased tissue oxygenation to sensitize some tumors to ionizing radiation (46–48). Our data shows that CD47 suppression protects vascular function after irradiation, so improved blood flow in the morpholino treated tumors may result in a greater re-growth delay due to increased oxygen-dependent free radical damage to these tumors (49). At present we have no data to support this as an acute mechanism to increase regrowth delay, but the laser Doppler data demonstrates that CD47 suppression preserves vascular responsiveness to NO when assessed 8 weeks after irradiation. Additional studies are needed to determine whether the same treatment acutely increases tumor perfusion and oxygenation.

Radiation therapy commonly results in lymphopenia, low functional activity of natural killer lymphocytes, decreased monocyte phagocytic activity, and decreased TNF-α production in cancer patients (50). TSP1 and CD47 are both implicated in phagocytic activity. TSP1 acts as a bridging molecule between phagocytes and apoptotic target cells (51,52), and CD47 expression on target cells limits their phagocytosis by engaging its counter-receptor SIRPα on phagocytic cells (53). A recent study of human myeloid leukemias found elevated CD47 expression and demonstrated that this can prevent macrophage-dependent clearance of the tumor cells in vivo (43). Thus, suppression by the morpholino of CD47 on tumor cells in our experiments may enhance their phagocytosis by M1-differentiated tumor macrophages, while suppression of CD47 on tumor infiltrating leukocytes may simultaneously preserve the viability and function of these cells after irradiation. This hypothesis is consistent with the reduced apoptosis of tumor infiltrating cells seen after irradiation following CD47 suppression. This resistance may enable the host innate immune cells in treated mice to better attack irradiated tumor cells.

Although we have only demonstrated in vivo efficacy of the antisense morpholino, in vitro studies demonstrate that the TSP1/CD47 pathway can also be targeted using monoclonal antibodies that bind to either TSP1 or CD47 and by small peptides that inhibit TSP1 binding to CD47 (29). Like the morpholino, these agents maintain cell viability and proliferative capacity after irradiation. Thus, these agents or orally available small molecules designed to inhibit TSP1 binding to CD47 could also be effective radioprotectants *in vivo* and merit further development. However, the CD47 morpholino also merits further investigation as a potential therapeutic based on our evidence that it has systemic activity to improve tumor responses to irradiation.

TSP1-CD47 antagonists are also known to limit physiologic NO signaling (28). Yet, our control experiments suggest that, in the case of radiation injury, cell protection from TSP1/CD47 blockade occurs primarily in an NO-independent manner. We do not yet know whether other known molecular targets of CD47 signaling such as Fas or G proteins are involved (54,55).

The single dose levels of radiation employed on both cultured cells and animal hindlimbs in this study are approximately 10-fold greater than the typical 1.8-2 Gy daily dose currently employed for radiotherapy of cancers and are within the 20–80 Gy total doses used for such treatment (56). Nevertheless, TSP1/CD47 blockade renders isolated cells and composite tissue nearly immune to radiation induced cell death and tissue necrosis/damage. These findings indicate that agents targeting TSP1/CD47 may allow for more aggressive application of radiation in the treatment of cancer and increase the percentage of curative responses.

Materials and Methods

Reagents and cells

HUVEC were cultured in endothelial basal medium supplemented with the manufacturer's additives and 2% fetal calf serum (FCS) in 5% CO_2 at 37° C (Lonza, Switzerland). The murine B16F10 melanoma was from Dr. L. Varticovski (NCI). The squamous cell carcinoma cell line SCC VII was as described (57). Cells were expanded in standard growth medium (RPMI 1640 with 10% FCS; Gibco, Grand Island, NY), screened for rodent viruses, and frozen at uniform passage for injection in mice. A CD47 targeting morpholino oligonucleotide (5′-CGTCACAGGCAGGACCCACTGCCCA) and mismatched control morpholino, a CD36 targeting morpholino (5′-ATGGGCTGTGACCGGAACTGTGGGC-3′) and a 4 base mismatched control, and Endoporter delivery vehicle were purchased from GeneTools (Philmonth, Oregon). The CD47 targeting morpholino blocks translation of both murine and human CD47 mRNAs (58). Mouse monoclonal antibodies recognizing human CD47 (B6H12) and murine or human TSP1 (A6.1) were purchased from Abcam (Cambridge, MA). The TSP1-

derived CD47 binding peptide FIRVVMYEGKK (7N3) was synthesized by Peptides International (Louisville, KY). A control peptide FIRGGMYEGKK (604) was synthesized by the late H. Krutzsch (NCI, NIH) (59). NG-nitro-L-arginine methyl ester (L-NAME) and the cGMP analog 8-Bromo cGMP were obtained from Sigma (St. Louis, MO). DETA/NO and DEA/NO were synthesized by Dr. L. Keefer (NCI, Frederick, MD).

Animals

C57BL/6 and C3H mice were housed in a pathogen-free environment and had ad libitum access to rat chow and water. Care and handling of animals under protocol LP-012 was in compliance with standards established by the Animal Use and Care Committee of the National Cancer Institute.

Irradiation of mice

Age and sex matched wild type mice underwent local irradiation to the right hindlimb as described (27). Forty-eight hours prior to irradiation, animals received the CD47 morpholino, a control morpholino (both at 10 μM in 750 μl PBS via intramuscular injection), vehicle, or no treatment to the hindlimb. Under 1% isoflurane inhalation anesthesia, the animals were placed in customized Lucite jigs that allow for immobilization and selective irradiation of the right hindlimb. A single radiation dose of 25 Gy was delivered by a Therapax DXT300 X-ray irradiator (Pantak, Inc., East Haven, CT) using 2.0-mm Al filtration (300 kVp) at a dose rate of 2.53 Gy/min. Care was taken to avoid irradiation of other body parts by using lead shields specifically designed as a part of the jigs. After irradiation, the animals were placed in cages as indicated above and observed weekly. Skin reaction after hindlimb irradiation was quantified every week after treatment for 8 weeks using a previously described grading system (60). Briefly, the tissue necrosis grading system consists of 5 categories: normal, hair loss, erythema, dry desquamation, and moist desquamation/ulceration. Leg contraction was assessed as described (27).

In other experiments, mice were injected in the right hindlimb with either 1×10^6 B16F10 melanoma cells (C57BL/6 mice) or 1.5×10^5 SCC VII cells (C3H mice), and tumors were allowed to grow for 1 week. After tumor incorporation, the hindlimbs were treated by local subcutaneous/intramuscular injection with either the CD47 morpholino (10 μM in sterile PBS) or an equal volume of PBS or by intraperitonal injection of the CD47 morpholino. Forty-eight hours later, all mice were subjected to right hindlimb irradiation (10 Gy). The mice were observed and tumor size determined two to three times a week by the same individual until lesion size necessitated animal euthanasia.

Irradiation of cells

HUVEC and B16 mouse melanoma cells were plated in standard growth medium in 96- or 6-well culture plates (Nunc) and allowed to adhere. Irradiation was done on a Precision X-Ray X-Rad 320 (East Haven, CT) operating at 300 kV/10 mA with a 2 mm aluminum filter. The dose rate at 50 cm from the x-ray source was 242 cGy/minute, as determined by multiple thermoluminescent dosimeter readings.

Cell Viability Assay

HUVEC were plated at a density of 5000 cells/well in 96 well plates (Nunc) and treated 24 hours later with the indicated doses of an anti-human CD47 antibody (B6H12), a TSP1 antibody (A6.1), the CD47-binding peptide 7N3, or control peptide 604. One hour later the cells were exposed to a single dose of gamma radiation (0, 10, 20, 30, and 40 Gy) and allowed to incubate another 72 hours at 37°C. Experiments with B16 melanoma cells were done in a similar manner treating either 1 hour prior to a single dose of radiation (10 Gy) with peptide 7N3 or 48 hours

prior with CD47 morpholino. Cell viability was determined by [3-(4,5-dimethylthiazol-2-yl)-5-(3-carboxymethoxyphenyl)-2-(4-sulfophenyl)-2H-tetrazolium (MTS) reduction using the CellTiter 96 Aqueous One Solution cell proliferation assay (Promega, Madison, WI) as per the manufacturer's instructions, and absorbance at 490 nm was determined with a plate reader (Dynatech, Alexandria, VA). The same assay was performed on HUVEC treated with either the CD47 or CD36 morpholino, but 48 h were allowed to pass prior to radiation (0 or 40 Gy) to allow for suppression of the target proteins. Similarly, control experiments were performed using the nitric oxide synthase inhibitor L-NAME, a membrane permeable cGMP analog, 8-Bromo cGMP, or the NO donor DETA/NO.

Cellular Proliferation Assay

Proliferation was assessed by quantifying incorporation of bromodeoxyuridine (BrdU) into newly synthesized DNA with a BrdU cell proliferation assay (Calbiochem, La Jolla, CA) performed as described (27).

Tissue Apoptosis

The ApopTag *in situ* detection kit (Chemicon, Millipore, MA) was used following the manufacturer's recommendations and performed as described (27). In brief, animals were sacrificed 24 h post irradiation (25 Gy) and hindlimbs embedded in paraffin blocks (American HistoLabs, Gaithersburg, MD). In other experiments, animals were injected with 1×10^6 B16 melanoma cells and treated with either CD47 morpholino or sterile PBS as above. Mice were sacrificed 24 h after irradiation (10 Gy), and hindlimbs were embedded in paraffin blocks. Tissue sections incorporating the entire hindlimb were examined for apoptosis employing 3′-hydroxy DNA strand breaks enzymatically labeled with digoxygenin nucleotide via TdT. Positive and negative control slides provided with the kit were used in each assay to ensure consistency.

Hematopoietic progenitor colony-forming assay

C57BL/6 mice, 8–10 weeks old were exposed to 10 Gy of irradiation to the hindlimb as described above. Mice were injected IP with equal volumes of PBS or 10 μM CD47 morpholino in 750 μl of PBS 48 h prior to irradiation. Immediately after irradiation, the mice were euthanized by cervical dislocation, and femurs were extracted from the irradiated hindlimbs under aseptic conditions. The femoral bone was cut at both joint ends, and a single cell suspension of bone marrow cells from each individual mouse was obtained by flushing the femoral cavity with 5 mL of cold RPMI containing 2% fetal calf serum using a 22-gauge needle. The suspension of bone marrow cells was filtered through a 40 μm nylon mesh cell strainer (Falcon, Becton Dickson Franklin Lakes, NJ USA) and centrifuged at 400 g for 10 min at 4° C. Cells were plated in triplicate from each mouse in 35 mm dishes at a density of 2×10^4/ml mixed with 1 ml of semisolid methylcellulose medium (Methocult M3434 Stem Cell Technologies, Vancouver, BC, Canada) containing murine recombinant erythropoietin, stem cell factor, interleukin 6, and interleukin-3 to support the formation of CFU-E, BFU-E, CFU-G, CFU-M, CFU-GM, and CFU-GEMM. Cultures were grown in a humidified 37°C incubator with 5% CO_2 in air, and colonies of more that 30 cells were counted on day 10.

Laser Doppler Analysis

Hindlimb blood flow was measured with laser Doppler imaging (MoorLD1-2; Moor Instruments, Devon, UK) as described (24,61). Animals received 25 Gy to right and left hindlimbs. The right limb also received 500 μl of 10 μM CD47 morpholino in sterile PBS via intramuscular injection 48 hours prior to radiation. Analysis of hindlimb blood flow to vasoactive challenge was performed 8 weeks later. Studies were performed under 1.5% isoflurane inhalation anesthesia and at a core temperature of 36.5° C. The parameters of the

scan area; 1.6 × 2.5 cm, scan speed; 4 ms per pixel, scan time; 1 minute 54 sec, override distance; 20 cm. After obtaining baseline analysis of limb blood flow, an NO challenge (10 μM DEA/NO, 100 nmol/g bodyweight) was administered via intra-rectal instillation and flow analysis repeated. Blood flow was quantified by integrating flux measurements over the area of interest at each time point and normalized to baseline integrated flux for the same limb in each mouse.

Immunohistochemical Evaluation

Staining for the macrophage marker CD68 was done as previously described (62) utilizing a rat anti-mouse CD68 antibody (AbD Serotec, Raleigh, NC). H&E staining of tissue hindlimbs was prepared by American HistoLabs, Gaithersburg, MD.

Statistics

Results are presented as the mean ± SD with significance calculated by the Student's *t* test or ANOVA analysis as appropriate using a standard software package (OriginLab Corporation, Northampton, MA). Significance was assigned for a P value$\leq$0.05.

Supplementary Material

Refer to Web version on PubMed Central for supplementary material.

References

1. Nair CK, Parida DK, Nomura T. Radioprotectors in radiotherapy. J Radiat Res (Tokyo) 2001;42:21–37. [PubMed: 11393887]
2. Emami B, et al. Tolerance of normal tissue to therapeutic irradiation. Int J Radiat Oncol Biol Phys 1991;21:109–122. [PubMed: 2032882]
3. Stone HB, Coleman CN, Anscher MS, McBride WH. Effects of radiation on normal tissue: consequences and mechanisms. Lancet Oncol 2003;4:529–536. [PubMed: 12965273]
4. Duchstein S, Gademann G, Peters B. Early and late effects of local high dose radiotherapy of the brain on memory and attention. Strahlenther Onkol 2003;179:441–451. [PubMed: 12835880]
5. Coleman CN. Radiation oncology--linking technology and biology in the treatment of cancer. Acta Oncol 2002;41:6–13. [PubMed: 11990520]
6. Ebert MA. Optimisation in radiotherapy I: defining the problem. Australas Phys Eng Sci Med 1997;20:164–176. [PubMed: 9409017]
7. Baker DG, Krochak RJ. The response of the microvascular system to radiation: a review. Cancer Invest 1989;7:287–294. [PubMed: 2477120]
8. Spitz DR, Azzam EI, Li JJ, Gius D. Metabolic oxidation/reduction reactions and cellular responses to ionizing radiation: a unifying concept in stress response biology. Cancer Metastasis Rev 2004;23:311–322. [PubMed: 15197331]
9. Goodhead DT. Initial events in the cellular effects of ionizing radiations: clustered damage in DNA. Int J Radiat Biol 1994;65:7–17. [PubMed: 7905912]
10. Cann KL, Hicks GG. Regulation of the cellular DNA double-strand break response. Biochem Cell Biol 2007;85:663–674. [PubMed: 18059525]
11. Bertram C, Hass R. Cellular responses to reactive oxygen species-induced DNA damage and aging. Biol Chem 2008;389:211–220. [PubMed: 18208352]
12. Katz D, Ito E, Liu FF. On the path to seeking novel radiosensitizers. Int J Radiat Oncol Biol Phys 2009;73:988–996. [PubMed: 19251086]
13. Weiss JF, Landauer MR. History and development of radiation-protective agents. Int J Radiat Biol 2009;85:539–573. [PubMed: 19557599]
14. Sasse AD, Clark LG, Sasse EC, Clark OA. Amifostine reduces side effects and improves complete response rate during radiotherapy: results of a meta-analysis. Int J Radiat Oncol Biol Phys 2006;64:784–791. [PubMed: 16198504]

15. Cassatt DR, Fazenbaker CA, Bachy CM, Hanson MS. Preclinical modeling of improved amifostine (Ethyol) use in radiation therapy. Semin Radiat Oncol 2002;12:97–102. [PubMed: 11917293]
16. Cassatt DR, Fazenbaker CA, Kifle G, Bachy CM. Preclinical studies on the radioprotective efficacy and pharmacokinetics of subcutaneously administered amifostine. Semin Oncol 2002;29:2–8. [PubMed: 12577236]
17. Greenberger JS. Radioprotection. In Vivo 2009;23:323–336. [PubMed: 19414422]
18. Isenberg JS, Wink DA, Roberts DD. Thrombospondin-1 antagonizes nitric oxide-stimulated vascular smooth muscle cell responses. Cardiovasc Res 2006;71:785–793. [PubMed: 16820142]
19. Chen H, Herndon ME, Lawler J. The cell biology of thrombospondin-1. Matrix Biol 2000;19:597–614. [PubMed: 11102749]
20. Isenberg JS, et al. Thrombospondin-1 inhibits endothelial cell responses to nitric oxide in a cGMP-dependent manner. Proc Natl Acad Sci U S A 2005;102:13141–13146. [PubMed: 16150726]
21. Isenberg JS, et al. CD47 is necessary for inhibition of nitric oxide-stimulated vascular cell responses by thrombospondin-1. J Biol Chem 2006;281:26069–26080. [PubMed: 16835222]
22. Isenberg JS, et al. Thrombospondin-1 stimulates platelet aggregation by blocking the antithrombotic activity of nitric oxide/cGMP signaling. Blood 2008;111:613–623. [PubMed: 17890448]
23. Isenberg JS, et al. Treatment of liver ischemia-reperfusion injury by limiting thrombospondin-1/CD47 signaling. Surgery 2008;144:752–761. [PubMed: 19081017]
24. Isenberg JS, et al. Blocking thrombospondin-1/CD47 signaling alleviates deleterious effects of aging on tissue responses to ischemia. Arterioscler Thromb Vasc Biol 2007;27:2582–2588. [PubMed: 17916772]
25. Wink DA, et al. Nitric oxide protects against cellular damage and cytotoxicity from reactive oxygen species. Proc Natl Acad Sci U S A 1993;90:9813–9817. [PubMed: 8234317]
26. Liebmann J, et al. In vivo radiation protection by nitric oxide modulation. Cancer Res 1994;54:3365–3368. [PubMed: 7516820]
27. Isenberg JS, et al. Thrombospondin-1 and CD47 limit cell and tissue survival of radiation injury. Am J Pathol 2008;173:1100–1112. [PubMed: 18787106]
28. Isenberg JS, et al. Thrombospondin-1 inhibits nitric oxide signaling via CD36 by inhibiting myristic acid uptake. J Biol Chem 2007;282:15404–15415. [PubMed: 17416590]
29. Isenberg JS, et al. Differential interactions of thrombospondin-1, -2, and -4 with CD47 and effects on cGMP signaling and ischemic injury responses. J Biol Chem 2009;284:1116–1125. [PubMed: 19004835]
30. Isenberg JS, et al. Blockade of thrombospondin-1-CD47 interactions prevents necrosis of full thickness skin grafts. Ann Surg 2008;247:180–190. [PubMed: 18156939]
31. Isenberg JS, et al. Gene silencing of CD47 and antibody ligation of thrombospondin-1 enhance ischemic tissue survival in a porcine model: implications for human disease. Ann Surg 2008;247:860–868. [PubMed: 18438125]
32. Isenberg JS, et al. Thrombospondin-1 limits ischemic tissue survival by inhibiting nitric oxide-mediated vascular smooth muscle relaxation. Blood 2007;109:1945–1952. [PubMed: 17082319]
33. Mouthon MA, Vereycken-Holler V, Van der Meeren A, Gaugler MH. Irradiation increases the interactions of platelets with the endothelium in vivo: analysis by intravital microscopy. Radiat Res 2003;160:593–599. [PubMed: 14565822]
34. Milliat F, et al. Influence of endothelial cells on vascular smooth muscle cells phenotype after irradiation: implication in radiation-induced vascular damages. Am J Pathol 2006;169:1484–1495. [PubMed: 17003501]
35. Garcia-Barros M, et al. Tumor response to radiotherapy regulated by endothelial cell apoptosis. Science 2003;300:1155–1159. [PubMed: 12750523]
36. Isenberg, JS.; Frazier, WA.; Roberts, DD. Cell and Gene Therapy. Templeton, NS., editor. CRC Press; 2008. p. 487-496.
37. Mantovani A, Sica A, Locati M. New vistas on macrophage differentiation and activation. Eur J Immunol 2007;37:14–16. [PubMed: 17183610]
38. Pollard JW. Tumour-educated macrophages promote tumour progression and metastasis. Nat Rev Cancer 2004;4:71–78. [PubMed: 14708027]

39. Nakakubo Y, et al. Clinical significance of immune cell infiltration within gallbladder cancer. Br J Cancer 2003;89:1736–1742. [PubMed: 14583778]
40. Matozaki T, Murata Y, Okazawa H, Ohnishi H. Functions and molecular mechanisms of the CD47-SIRPalpha signalling pathway. Trends Cell Biol 2009;19:72–80. [PubMed: 19144521]
41. Okazawa H, et al. Negative regulation of phagocytosis in macrophages by the CD47-SHPS-1 system. J Immunol 2005;174:2004–2011. [PubMed: 15699129]
42. Ide K, et al. Role for CD47-SIRPalpha signaling in xenograft rejection by macrophages. Proc Natl Acad Sci U S A 2007;104:5062–5066. [PubMed: 17360380]
43. Jaiswal S, et al. CD47 is upregulated on circulating hematopoietic stem cells and leukemia cells to avoid phagocytosis. Cell 2009;138:271–285. [PubMed: 19632178]
44. Matsumura S, et al. Radiation-induced CXCL16 release by breast cancer cells attracts effector T cells. J Immunol 2008;181:3099–3107. [PubMed: 18713980]
45. Friedman EJ. Immune modulation by ionizing radiation and its implications for cancer immunotherapy. Curr Pharm Des 2002;8:1765–1780. [PubMed: 12171547]
46. Feldmann HJ. Oxygenation of human tumors--implications for combined therapy. Lung Cancer 2001;33(Suppl 1):S77–83. [PubMed: 11576711]
47. Bourke VA, et al. Correlation of radiation response with tumor oxygenation in the Dunning prostate R3327-AT1 tumor. Int J Radiat Oncol Biol Phys 2007;67:1179–1186. [PubMed: 17336219]
48. Bennett M, Feldmeier J, Smee R, Milross C. Hyperbaric oxygenation for tumour sensitisation to radiotherapy: a systematic review of randomised controlled trials. Cancer Treat Rev 2008;34:577–591. [PubMed: 18640781]
49. Molls M, Stadler P, Becker A, Feldmann HJ, Dunst J. Relevance of oxygen in radiation oncology. Mechanisms of action, correlation to low hemoglobin levels. Strahlenther Onkol 1998;174(Suppl 4): 13–16. [PubMed: 9879341]
50. Gonzalez-Angulo AM, Morales-Vasquez F, Hortobagyi GN. Overview of resistance to systemic therapy in patients with breast cancer. Adv Exp Med Biol 2007;608:1–22. [PubMed: 17993229]
51. Krispin A, et al. Apoptotic cell thrombospondin-1 and heparin-binding domain lead to dendritic-cell phagocytic and tolerizing states. Blood 2006;108:3580–3589. [PubMed: 16882710]
52. Savill J. Recognition and phagocytosis of cells undergoing apoptosis. Br Med Bull 1997;53:491–508. [PubMed: 9374033]
53. Olsson M, Oldenborg PA. CD47 on experimentally senescent murine RBCs inhibits phagocytosis following Fcgamma receptor-mediated but not scavenger receptor-mediated recognition by macrophages. Blood 2008;112:4259–4267. [PubMed: 18779391]
54. Manna PP, Frazier WA. CD47 mediates killing of breast tumor cells via Gi-dependent inhibition of protein kinase A. Cancer Res 2004;64:1026–1036. [PubMed: 14871834]
55. Manna PP, Dimitry J, Oldenborg PA, Frazier WA. CD47 augments Fas/CD95-mediated apoptosis. J Biol Chem 2005;280:29637–29644. [PubMed: 15917238]
56. Chao, KSC.; Perez, CA.; Brady, LW. Radiation oncology: management decisions. Lippincott Williams & Wilkins; Philadelphia: 2002.
57. Cook JA, et al. Radiation-induced changes in gene-expression profiles for the SCC VII tumor cells grown in vitro and in vivo. Antioxid Redox Signal 2006;8:1263–1272. [PubMed: 16910774]
58. Isenberg JS, et al. Increasing survival of ischemic tissue by targeting CD47. Circ Res 2007;100:712–720. [PubMed: 17293482]
59. Barazi HO, et al. Regulation of integrin function by CD47 ligands. Differential effects on αvβ3 and α4β1 integrin-mediated adhesion. J Biol Chem 2002;277:42859–42866. [PubMed: 12218055]
60. Flanders KC, et al. Interference with transforming growth factor-beta/Smad3 signaling results in accelerated healing of wounds in previously irradiated skin. Am J Pathol 2003;163:2247–2257. [PubMed: 14633599]
61. Isenberg JS, et al. Thrombospondin 1 and vasoactive agents indirectly alter tumor blood flow. Neoplasia 2008;10:886–896. [PubMed: 18670646]
62. Martin-Manso G, et al. Thrombospondin 1 promotes tumor macrophage recruitment and enhances tumor cell cytotoxicity of differentiated U937 cells. Cancer Res 2008;68:7090–7099. [PubMed: 18757424]

63. This work was supported by the Intramural Research Program of the National Institutes of Health, National Cancer Institute, Center for Cancer Research (D.D.R., D.A.W., M.T.), NIH grant K22 CA128616 (J.S.I.) and by the Howard Hughes Medical Institute-NIH Research Scholars Program (H.B.S.). We thank Drs. L. Varticovski and L. Keefer for providing reagents. J.B.M., D.S.P., J.S.I. performed experiments, interpreted data and wrote the manuscript; L.A.R., H.B.S., W.G.D. performed experiments and interpreted data; M.T., D.A.W., D.D.R. interpreted data and wrote the manuscript.

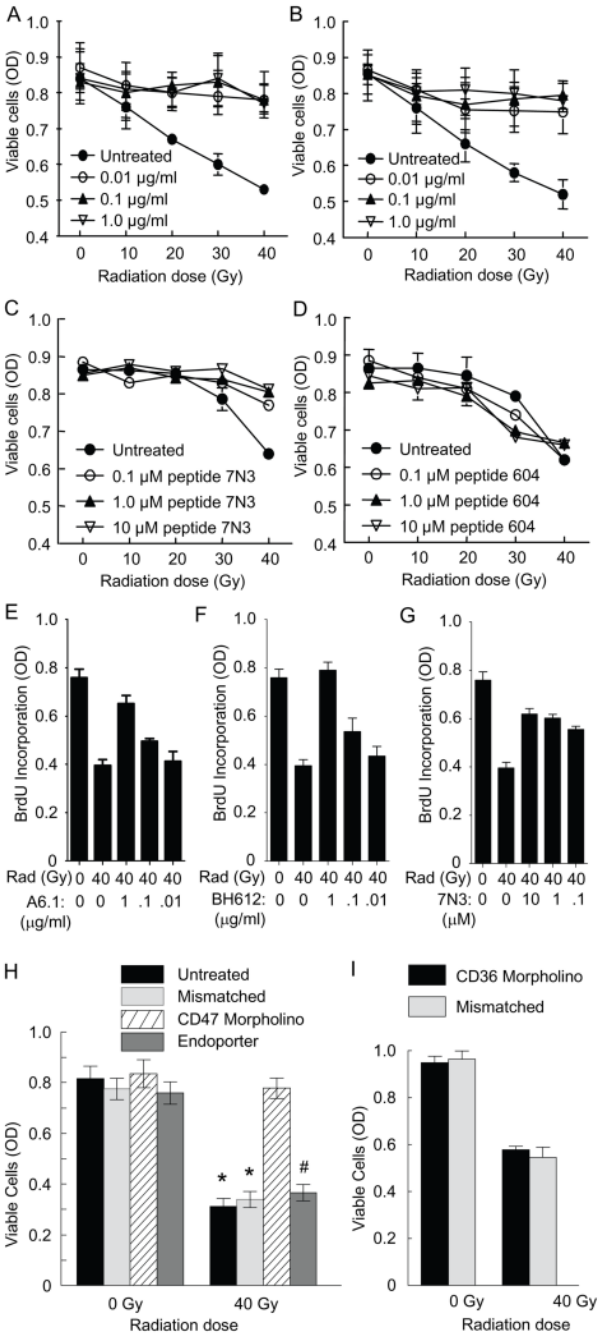

Fig. 1. Radioprotective activities of TSP1 and CD47 antibodies, a CD47 binding peptide from TSP1, and CD47 morpholino in human endothelial cells

HUVEC were treated with (A, E) TSP1 or (B, F) CD47 monoclonal antibodies (clone A6.1 or B6H12, respectively), (C, G) peptide 7N3, or (D) control peptide 604, and received the indicated doses of radiation 24 h after addition of the antibodies. Cell (mitochondrial) viability was measured 48 h after irradiation by MTS reduction (A–D), and cell proliferation was examined by BrdU incorporation into newly synthesized DNA (E–G). (H) Knockdown of CD47 by pretreatment of HUVEC for 48 h with a specific morpholino complexed with Endoporter vehicle protected against cell death as assessed by MTS reduction after a radiation dose of 40 Gy when compared to control groups (non-treated, mismatched morpholino

complexed with Endoporter, and Endoporter vehicle control) (*P <0.05, #P < 0.01). (I) Cells treated with a morpholino to suppress the TSP1 receptor CD36 under the same conditions demonstrated no radioprotection. Experiments were repeated 3 times, and results are presented as the mean optical density ± SD.

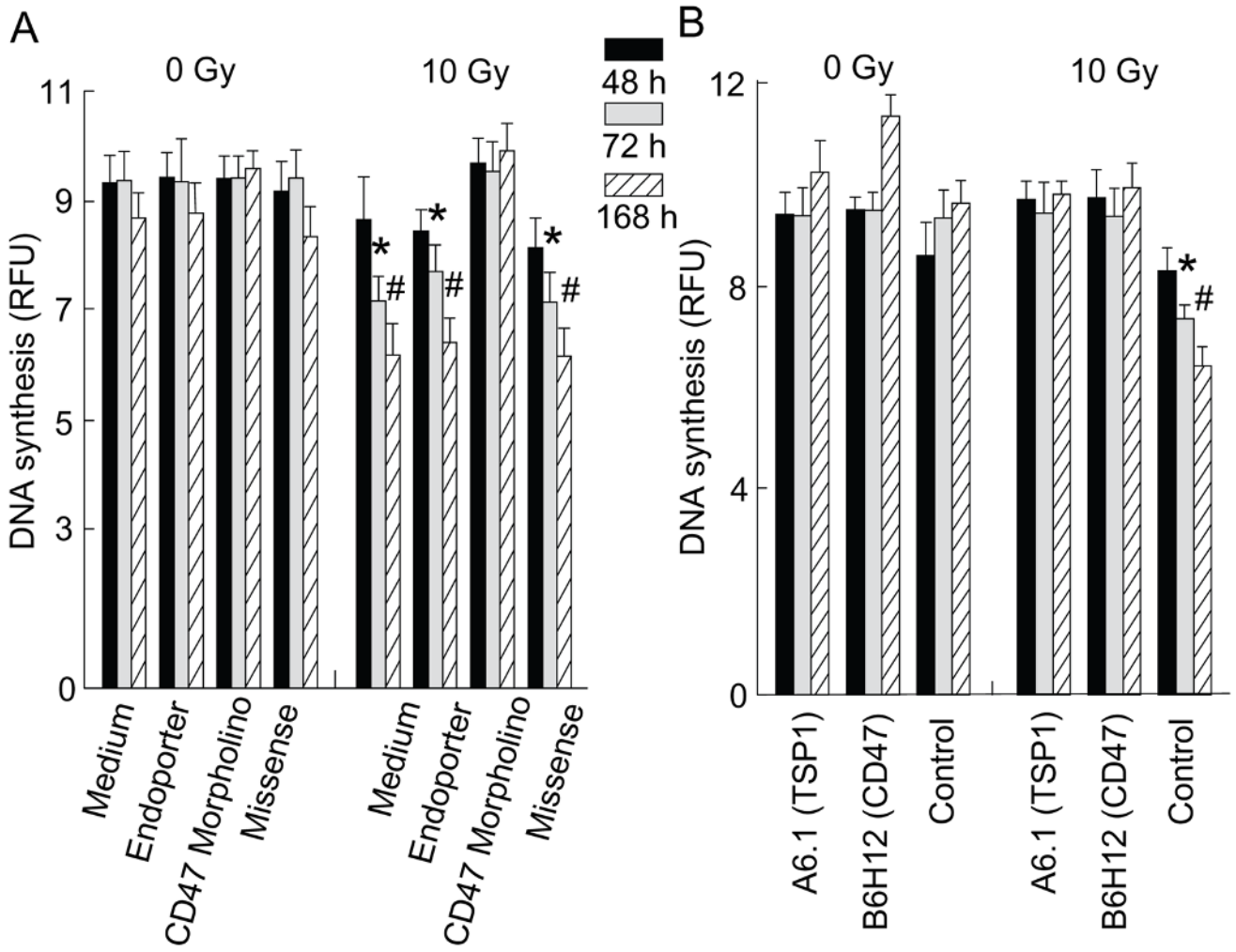

Fig. 2. Antibodies to TSP1 and CD47 and antisense suppression of CD47 maintain proliferation of irradiated human endothelial cells

HUVEC were treated with (A) CD47 morpholino or (B) TSP1 or CD47 antibodies and exposed to 10 Gy irradiation 48 hours later. DNA synthesis was assessed at the indicated times by BrdU incorporation, and relative fluorescence (RFU) is presented as the mean ± SD (*$P < 0.05$, #$p < 0.01$). Experiments were repeated 3 times.

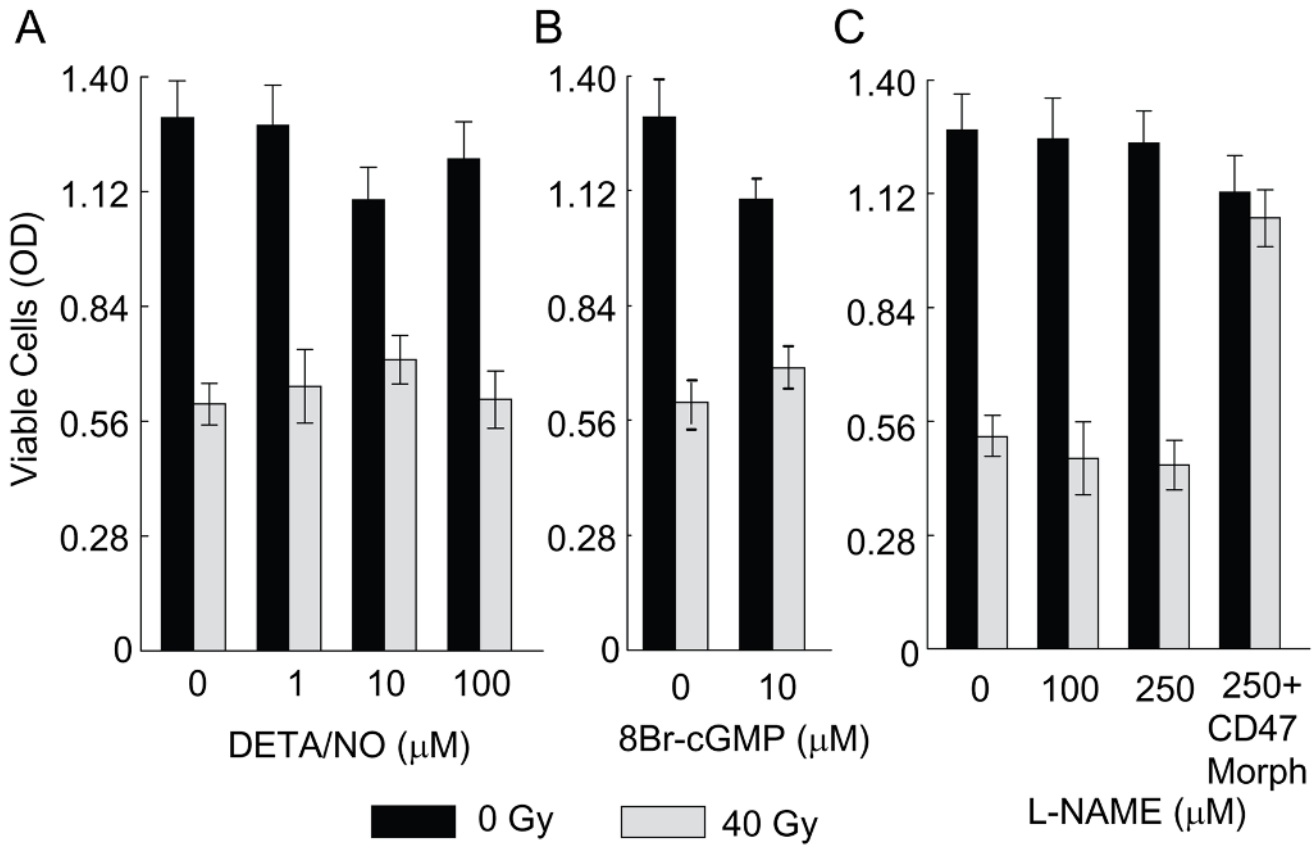

Fig. 3. The radioprotective effect of CD47 suppression is independent of NO/cGMP signaling

HUVEC were treated with the indicated doses of the slow releasing NO donor DETA/NO (A) or membrane permeable cGMP analog, 8-Bromo cGMP (B). Cell viability was measured by MTS reduction 48 hours after 40 Gy irradiation. (C) HUVEC or HUVEC treated with CD47 morpholino were incubated with the indicated concentrations of nitric oxide synthase inhibitor L-NAME prior to irradiation, and cell viability was measured by MTS reduction.

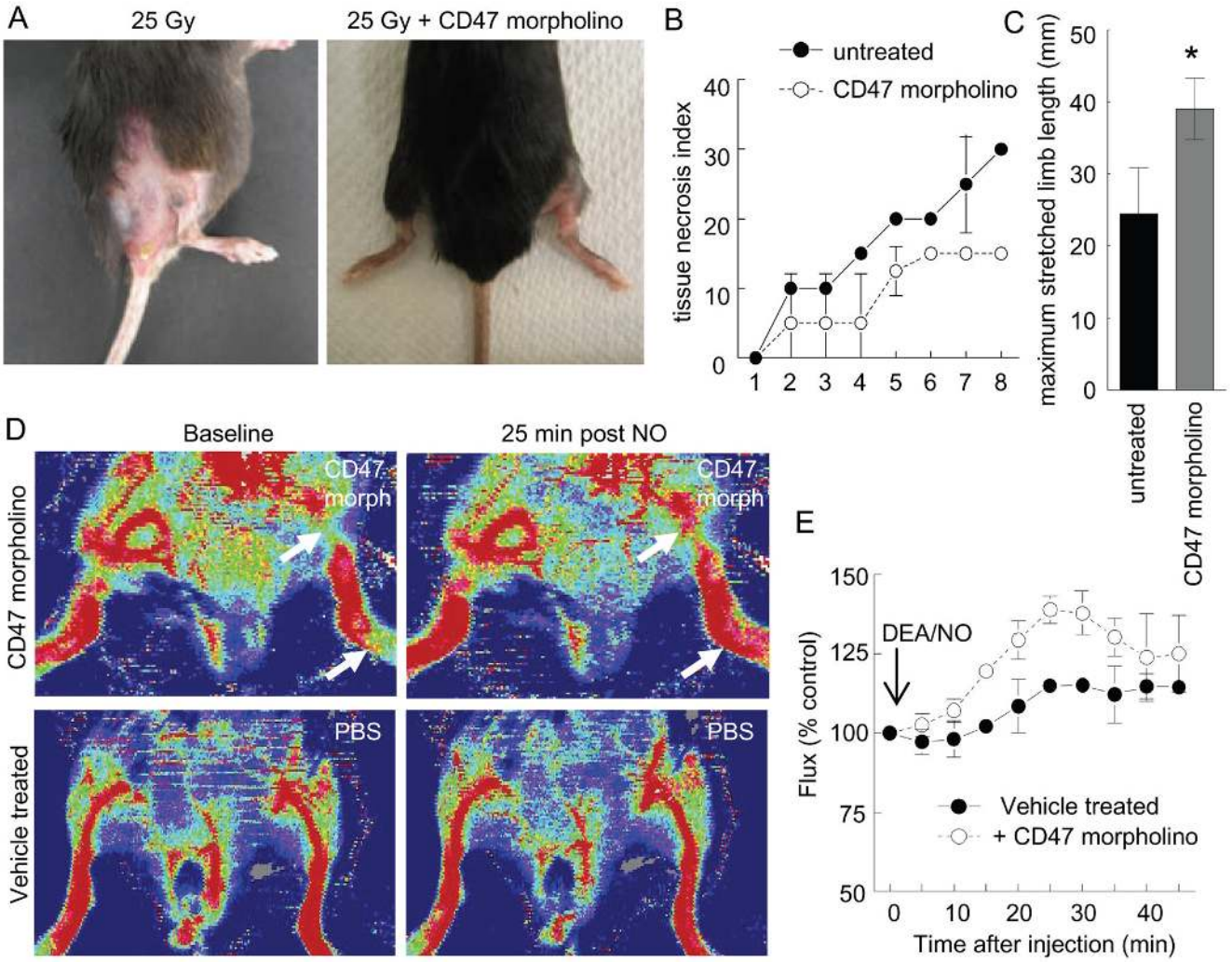

Fig. 4. CD47 suppression with an antisense morpholino minimizes tissue and vascular damage from radiation injury

Age and sex matched C57BL/6 wild type mice underwent a one-time treatment of the right hindlimb with either a CD47 morpholino oligonucleotide (10 μM in 750 μl PBS) or 750 μl of PBS only injected into the muscle and soft tissues and received 25 Gy irradiation to the treated hindlimb 48 hours later. (A) After 8 weeks, a representative image shows signs of fibrotic contractures only in the untreated irradiated hind limb. (B) Tissue necrosis grading scores for 8 animals were calculated weekly by assessing alopecia, ulceration, and desquamation and are presented as mean ± SD. (C) Fibrosis was assessed at 8 weeks by measuring hindlimb extension and is presented as mean ± SD (*$P < 0.05$). (D) C57BL/6 wild type mice were treated by direct intra-muscular injection of the right hindlimb with the CD47 morpholino (10 μM in 750 μl PBS, upper panels) or sterile PBS alone (lower panels) 48 hours prior to 25 Gy irradiation of both hindlimbs in each mouse. Eight weeks after radiation, right hindlimb blood flow responses to DEA/NO challenge (100 nmol/gram body weight via rectal instillation) were assessed via Laser Doppler imaging under 1.5% isoflurane inhalation anesthesia at a core temperature of 36.5° C. Representative images show a greater increase in blood flow after 25 min. in the right hindlimb of a morpholino treated mouse (arrows in upper panels) compared to the corresponding limb of a vehicle treated mouse (lower panels). (E) Blood flow velocity measurements (Flux) at the indicated time points were integrated over the area of the treated

hindlimbs of 6 mice in each group and normalized as a percent of the integrated baseline flux in the same limb of each mouse. Results are presented as the mean ± SD.

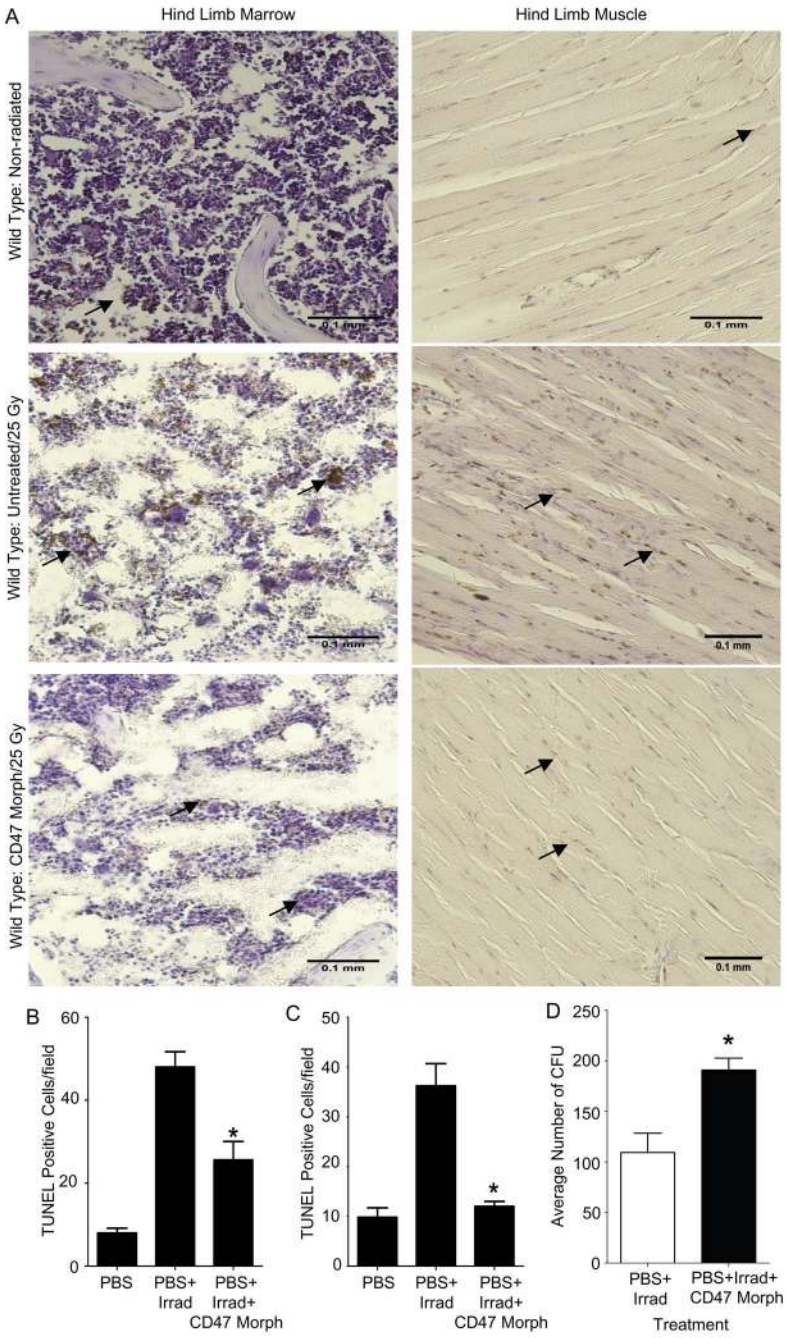

Fig. 5. Suppression of CD47 prevents radiation-induced apoptosis in muscle and bone marrow

(A) Un-irradiated control hindlimbs (upper panels) and hindlimbs irradiated at a dose of 25 Gy (middle and bottom panels) from age and sex matched C57BL/6 wild type mice were prepared for paraffin-embedded tissue sections 24 h post-radiation and stained for apoptotic nuclei by the TUNEL method (brown nuclear staining). Mouse hindlimbs injected with the CD47 morpholino (bottom panels) 48 h prior to radiation were also prepared in the same manner 24 h post-radiation. Apoptosis is inferred by intranuclear staining of muscle and bone marrow cells. Images were acquired using a 20x objective (B) Bone marrow apoptosis was quantified for 5 mice in each group and is presented as the average number of TUNEL positive cells in 3 tissue sections per animal (**P*<0.005). (C) Apoptosis in muscle was quantified for 5 mice in

each group and is presented as the average number of TUNEL positive cells in 3 tissue sections per animal (*P<0.001). (D) Assessment of colony forming units of haematopoietic progenitor cell derived from bone marrow cells of mice treated in the same manner as explained above. Data represent mean ± SEM of 6 mice per treatment group (*P<0.01).

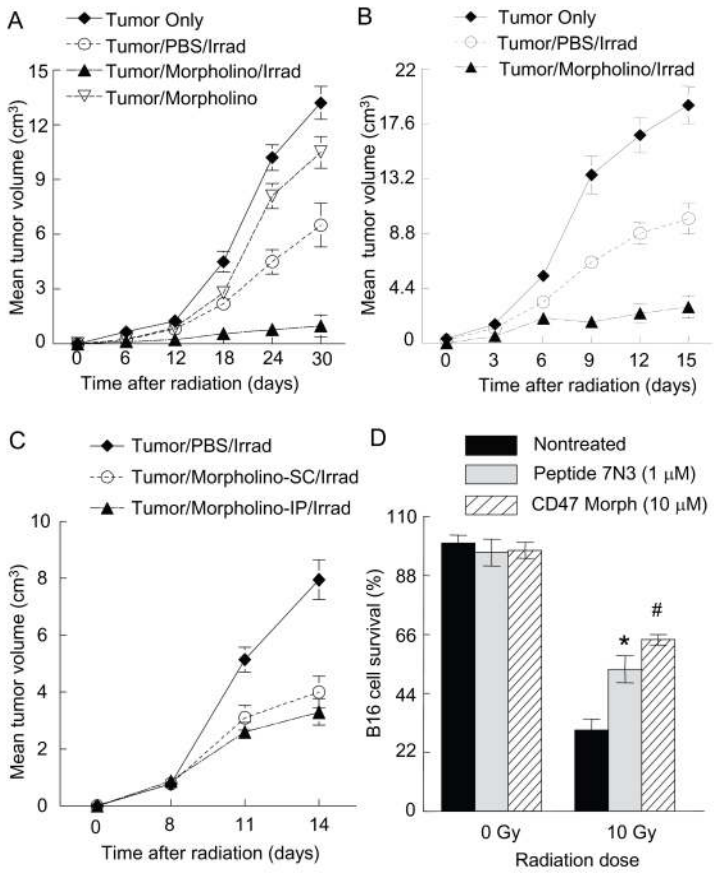

Fig. 6. CD47 suppression enhances re-growth delay in irradiated tumors but increases radioresistance of melanoma cells *in vitro*.

(A) C57BL/6 mice were injected with 1×10^6 B16 mouse melanoma cells into their right hindlimbs. Five days later, the mice were randomized into 4 groups (12 mice in each group) that received injections of CD47 morpholino (10 μM) in sterile PBS, PBS, or no injection. Two groups receiving injections were then subjected to radiation (10 Gy) to the affected hindlimb 48 h later. The other two groups served as controls. Tumor volume was measured every 6 days for 30 days. Results are presented as the mean ± SD of 12 mice in each treatment group and are representative of 3 independent studies. (B) The same experimental design was used to assess radiation delay for SCC VII squamous cell lung carcinoma tumors (SCC, 1.5×10^5 cells). Results are presented as the mean ± SD of 10 mice (C3H) in each treatment group and are representative of 3 independent studies. (C) Mice bearing SCC-VII tumors as in (B) were treated by local intramuscular and subcutaneous (SC) injections of PBS or CD47 morpholino or by intraperitoneal (IP) injection of CD47 morpholino, irradiated at 10 Gy, and tumor growth was assessed at the indicated times. (D) B16 melanoma cells plated on 96-well plates in standard growth medium were treated with peptide 7N3 or CD47 morpholino and received a radiation dose of 10 Gy. Cell (mitochondrial) viability was measured 48 h after radiation using the MTS assay (*P <0.05, #P < 0.01).

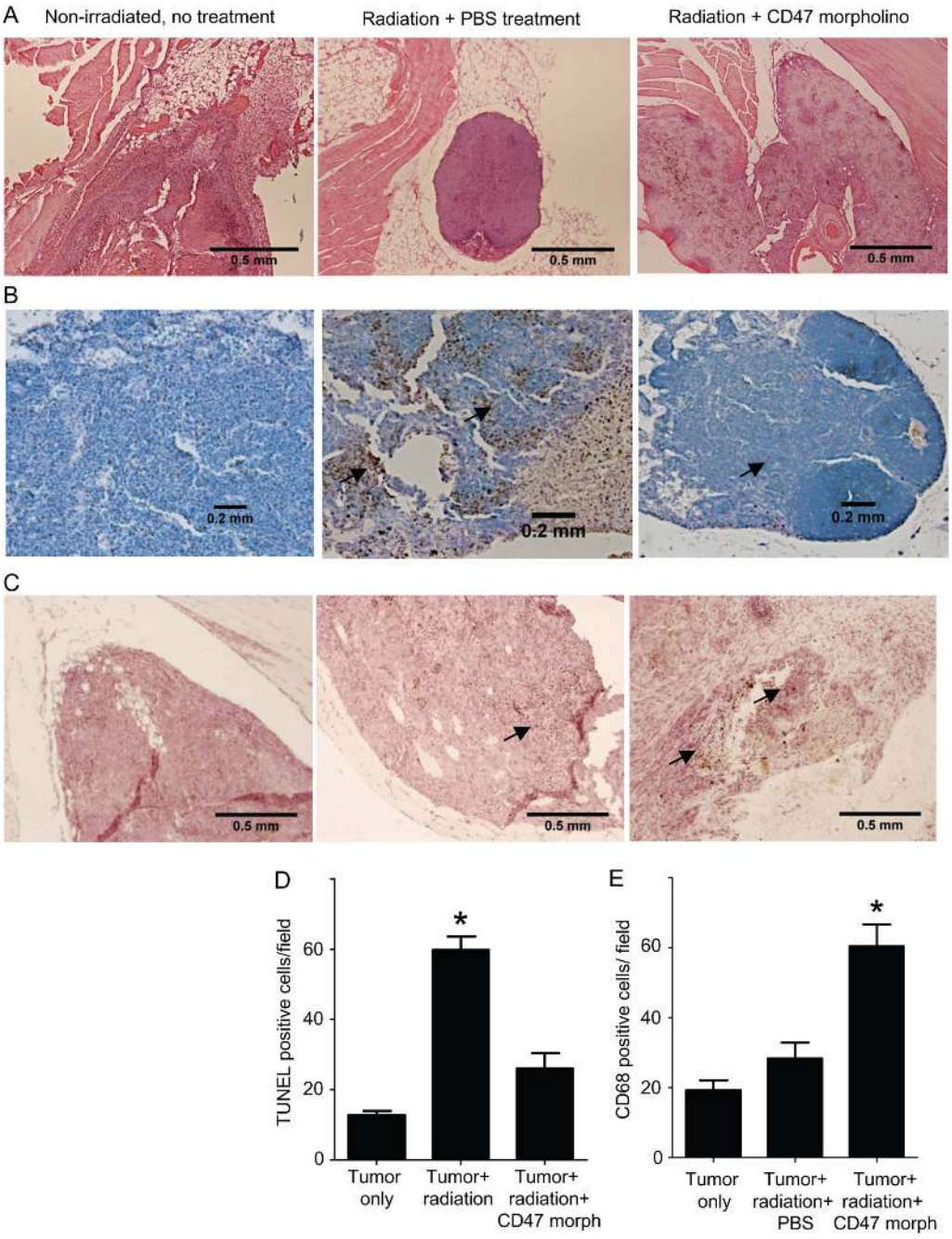

Fig. 7. Increased fibrotic response, viable leukocyte infiltrates, and macrophage infiltration in tumors with suppressed CD47 expression

C57BL/6 mice were injected with 1×10^6 B16 mouse melanoma cells into their hindlimbs. Treatment consisted of two groups in which the hindlimbs were treated with either 150 μl of PBS or 150 μl of CD47 morpholino (10 μM) 48 hours prior to radiation (10 Gy). The control group consisted of tumor without radiation. 24 h post-radiation the mice were sacrificed, and paraffin embedded tissue sections of the hindlimbs were prepared for analysis. (A) H&E stained sections of hindlimbs and tumors. (B) Detection of cells undergoing apoptosis by the TUNEL method. Apoptotic cells are indicated by brown nuclear staining (arrows). (C) Immunohistochemical staining for murine macrophage surface marker CD68. Dark brown

staining within the tumor indicates macrophage infiltration. Images were acquired using either a 4x or 10x objective. (D) Quantitative analysis of apoptotic tumor-associated cells by TUNEL staining, n= 5 in each group, $*P < 0.0001$) (E) Quantitative analysis of tumor-associated macrophages detected by CD68-immunostaining. (63)